ELSEVIER

Thermochimica Acta 398 (2003) 223–231

thermochimica acta

www.elsevier.com/locate/tca

# Investigation of solid–solid interactions in $NiO/Fe_2O_3$ system doped with ZnO

H.G. El-Shobaky [a,*], N.R.E. Radwan [b]

[a] *Department of Chemistry, Faculty of Science, Cairo University, Cairo, Egypt*
[b] *Department of Chemistry, Faculty of Education, Suez Canal University, Suez, Egypt*

Received 10 December 2001; received in revised form 19 June 2002; accepted 25 June 2002

## Abstract

The solid–solid interactions between pure and ZnO-doped nickel and ferric oxides have been investigated using DTA and XRD techniques. A mixture of equimolar proportions of finely powdered basic nickel carbonate and ferric oxide were impregnated with zinc nitrate dissolved in the minimum amount of distilled water making a paste. The paste was dried then calcined at 700–1100 °C. The amounts of dopant were 0.75, 1.5, 3 and 6 mol% ZnO.

The results obtained showed that the addition of zinc nitrate to the reacting mixed solids enhanced the thermal decomposition of nickel carbonate to an extent proportional to its amount added. $Fe_2O_3$ interacted readily with NiO at temperatures starting from 700 °C producing crystalline $NiFe_2O_4$ phase. The degree of reaction propagation increased as a function of temperature. However, heating of pure mixed solids at 1100 °C for 6 h did not affect the complete conversion of the reacting oxides to $NiFe_2O_4$. ZnO-doping of $NiO/Fe_2O_3$ system at 700–900 °C effected a limited enhancement in the formation of $NiFe_2O_4$. However, an effective enhancement of nickel ferrite was observed upon heating the doped solids at 1000–1100 °C. The activation energy of formation ($\Delta E$) of $NiFe_2O_4$ phase was determined for pure and doped solids by following up the change in the peak height of the diffraction line characteristic for $NiFe_2O_4$ at *d*-spacing 2.95 Å as a function of calcination temperature. The computed $\Delta E$ values were 103, 85, 70, 41 and 20 kJ mol$^{-1}$ for pure solids and those doped with 0.75, 1.5, 3 and 6 mol% ZnO, respectively. The decrease in $\Delta E$ value of $NiFe_2O_4$ formation as a function of dopant added was not only attributed to an effective increase in the mobility of the reacting cations but also to the formation of the mixed ferrite $Ni_{1-x}Zn_xFe_2O_4$ that substitute some of the early formed ferrite. The presence of this mixed ferrite led to an increase in the diffusion of the reacting cations through the ferrite film.

*Keywords:* XRD; Doping; $NiFe_2O_4$; Mobility; Activation energy; Nickel and Zn-ferrites

## 1. Introduction

The general chemical formula of a ferrite is $(M\,Fe_2O_4)_n$ where M represents a metallic cation. It is found that a spinel crystal structure is only formed if the ionic radius of the cation M is less than about 1 Å. If it is greater than 1 Å then the electrostatic coulomb forces are insufficient to ensure the stability of the crystal. The cation M is generally divalent, but other valences are possible if the number of anions is doubled. The ions forming ferrites of practical importance are $Ni^{2+}$, $Mn^{2+}$, $Fe^{2+}$, $Co^{2+}$, $Cu^{2+}$, $Zn^{2+}$, $Cd^{2+}$, $Li^{+}$, $Mg^{2+}$ [1–16]. The most likely arrangement of

---

[*] Corresponding author. Fax: +20-2-337-0931.
*E-mail address:* halla_elshobaky@yahoo.com (H.G. El-Shobaky).

0040-6031/03/$ – see front matter © 2002 Elsevier Science B.V. All rights reserved.
PII: S0040-6031(02)00368-4

the cations would be with $M^{2+}$ ions on the tetrahedral positions and $Fe^{3+}$ ions on the octahedral positions, but in practice three types of spinel can be distinguished: normal spinels in which $M^{2+}$ ions occupy the tetrahedral position and $Fe^{3+}$ the octahedral position; secondly inverse spinels in which $M^{2+}$ ions occupy the octahedral position together with half the $Fe^{3+}$ ions, the other half being on the tetrahedral position. The last type random spinels in which both $M^{2+}$ ions and $Fe^{3+}$ ions occur on the tetrahedral and octahedral positions. In general, normal ferrite spinels are paramagnetic while inverse spinels are ferromagnetic in nature.

Ferrites have found wide uses in many industrial applications and can be prepared either by ceramic or co-precipitation techniques depending on their end uses. The ferrite of similar composition differs in their magnetic properties depending on the preparation technique and particle size [17,18]. Several synthesis methods have been developed in order to obtain fine particles with controlled shapes and sizes [19–23] and particular magnetic properties [24–26]. Solid–solid interactions between ferric oxide and transition metal oxides or carbonates to produce the corresponding ferrites are much influenced by the prehistory of parent solids, their ratio and also by the addition of small amounts of certain foreign oxides [10–16,27–36]. The solid–solid interaction between $Fe_2O_3$ and transition metal oxides to produce the corresponding ferrite is normally controlled by the thermal diffusion of the reaction cations through the whole mass of each solid as well as the initially formed film covering the surface of the grains of each oxide [10–16,31,34] which act as energy barrier thus hindering their diffusion. So, the completion of these solid state reactions required a prolonged heating at relatively elevated temperatures [9–16,33,34]. The effect of $Li_2O$ and $Al_2O_3$ doping on the formation of $NiFe_2O_4$, $ZnFe_2O_4$ and $CoFe_2O_4$ formation were previously studied [10–16,31,34–36]. It was found that both $Li_2O$ and $Al_2O_3$ enhanced the ferrite formation with different degrees via increasing the mobility of thermal diffusion of reacting cations through the formed ferrite film.

The present work reports the results of a study on the effect of addition of small amounts of ZnO on nickel ferrite formation at different temperatures. The techniques employed were DTA and XRD.

## 2. Experimental

### 2.1. Materials

Equimolar mixtures of ferric oxide and basic nickel carbonate were well mixed to ensure the homogeneity of the powdered solids. The obtained sample was heated in air at temperatures 700, 900, 1000, 1050 and 1100 °C for 6 h. Four doped mixed solid samples were obtained by treating a known mass of mixed solids with calculated amount of zinc nitrate dissolved in the minimum amount of distilled water, dried at 100 °C, then calcined at 700, 900, 1000, 1050 and 1100 °C for 6 h. The concentration of zinc were 0.75, 1.5, 3 and 6 mol% ZnO. The chemicals employed in the present work were of analytical grade supplied by BDH.

### 2.2. Techniques

DTA curves of pure and doped uncalcined solid samples were determined using Shimadzu DTA-50H system. The rate of heating was kept at $10\,^{\circ}C\,min^{-1}$ and the mass of the solid specimen was 40 mg. The measurements was carried out in a current of dry air following at a rate of $50\,cm^3\,min^{-1}$.

An X-ray investigation of pure and variously doped mixed solids preheated in air at 700, 900, 1000, 1050 and 1100 °C was conducted using a Philips diffractometer (type Pw 1390). The patterns were run with iron-filtered cobalt radiation ($\lambda = 1.7889$ Å) at 30 kV and 10 mA with a scanning speed of $2\theta = 2^{\circ}\,min^{-1}$.

## 3. Results

### 3.1. Thermal behaviour of pure and doped uncalcined solids

Fig. 1 depicts the DTA curves of pure and $Zn(NO_3)_2$-doped uncalcined mixed solids ($Fe_2O_3$ and basic nickel carbonate). The DTA curves of pure mixed solids and those doped with 1.5 and 6 mol% $Zn(NO_3)_2$ consisted of three endothermic peaks. The first two peaks are weak and located at 45.3 and 65.4 °C. These peaks are indicative for the removal of water of crystallisation of basic nickel carbonate. The third peak was located at 295 °C. The sharpness of this peak increases as a function of the amount of zinc

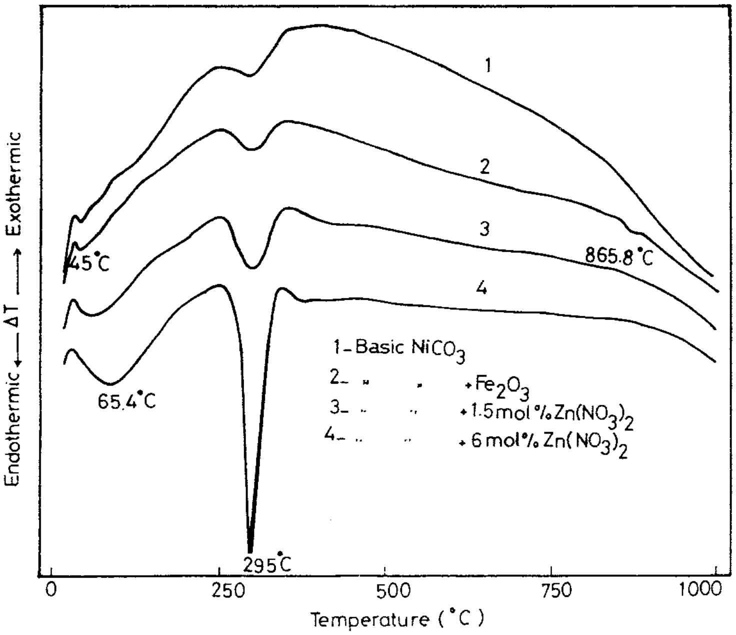

Fig. 1. DTA curves of pure and doped uncalcined mixed solids.

nitrate added. This indicates that $Zn(NO_3)_2$-doping increases the rate and/or the degree of nickel carbonate decomposition.

### *3.2. XRD investigation of pure and doped mixed solids precalcined at different temperatures*

X-ray diffractograms of pure and doped mixed solids precalcined at various temperatures were determined. The results obtained showed that pure and doped mixed oxide solids precalcined in air at 700 °C consisted mainly of $\alpha$-$Fe_2O_3$ and NiO phases. The diffraction patterns of pure and 0.75 mol% ZnO-doped sample are given in Fig. 2. The characteristic diffraction lines of nickel ferrite of high intensity at *d*-spacing of 2.51 Å (100%) and 1.48 Å (40%) are common between $\alpha$-$Fe_2O_3$ and both free oxides, respectively. So, once-over to these lines, it is difficult to talk about the possibility of solid–solid interaction between $\alpha$-$Fe_2O_3$ and NiO with subsequent production of $NiFe_2O_4$ crystalline phase. Preliminary experiments showed that the ratio between the peak height of the diffraction line at *d*-spacing 2.51 Å (100% $NiFe_2O_4$ and 50% $\alpha$-$Fe_2O_3$) to that of the line at 2.69 Å (100% $\alpha$-$Fe_2O_3$) in diffraction patterns of pure mixed solids precalcined at 600 °C was 0.55. This value is very close to that characteristic for $\alpha$-$Fe_2O_3$ phase. The values of the ratio (*R*) greater than 0.5 might be indicative for the probability of presence of $NiFe_2O_4$ phase. The variation of the peak heights of the diffraction lines at 2.51 and 2.69 Å and the ratio (*R*) between them are given in Table 1.

For the results given in Table 1 for pure and doped mixed oxide solids precalcined at 700 °C, the ratio (*R*) exceed 0.5. These results denote to the existence of $NiFe_2O_4$ crystalline phase. The ratio (*R*) is 0.725 for the pure sample, and exceeds 0.82 upon doping with ZnO (0.75–6 mol%). This indicates that doping of $NiO/Fe_2O_3$ system with ZnO followed by heating at 700 °C, enhances the solid–solid interactions between the free oxides yielding $NiFe_2O_4$. This enhancement may be attributed to the solubility of ZnO in both crystal lattices of the free oxides. The limited enhancement may suggest the limited solubility of ZnO at 700 °C in both free oxide lattices.

The X-ray diffractograms of pure and doped mixed oxide solids precalcined in air at 900 °C are similar. Only the diffraction patterns of pure sample and those doped with 0.75 and 1.5 mol% ZnO samples are given

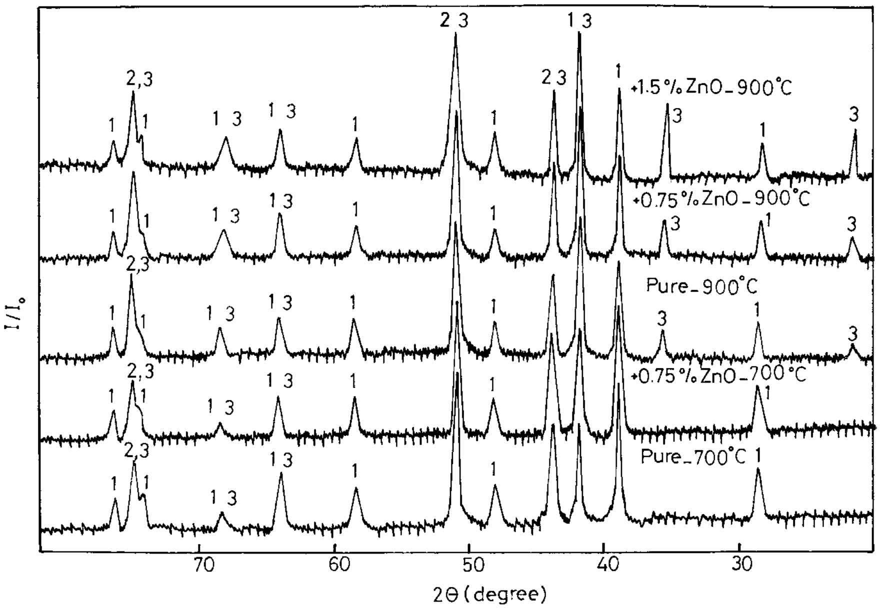

Fig. 2. X-ray diffractograms of pure and doped solids precalcined at 700 and 900 °C. Lines (1) α-$Fe_2O_3$, (2) NiO and (3) $NiFe_2O_4$.

in Fig. 2. This figure shows that these diffractograms consisted, mainly of α-$Fe_2O_3$, NiO beside the appearance of new diffraction lines at *d*-spacing 4.82 and 2.95 Å. These lines are characteristic or key-lines suggested by El-Shobaky et al. [31] for $NiFe_2O_4$ phase. The variation of the peak height at 2.95 Å (30% $NiFe_2O_4$) is given in the last column of Table 1. Inspection of Fig. 2, revealed that, for pure and doped mixed oxide solids precalcined at 900 °C, the peak height of the diffraction line at 2.69 Å decreases progressively as a function of the amount of ZnO added up to 1.5 mol% ZnO with subsequent increase in the peak height of the key-line. It is difficult to talk about the variation of the peak height of the diffraction lines characteristic for NiO or those characteristics for α-$Fe_2O_3$ other than 2.69 Å, because all of them are common with $NiFe_2O_4$. The variation in the peak heights at 2.69, 2.95 and 4.82 Å is confirmed by the increase in the ratio (*R*) given in Table 2 from 1.43 to 1.58 upon doping with 1.5 mol% ZnO. The ceiling values in the (*R*) due to doping with 1.5 mol% ZnO at 1.58 may reflect the limited solubility of ZnO in both α-$Fe_2O_3$ and NiO lattices. The (*R*) value given in Table 1 increases from 0.725 to 1.43 by increasing the precalcination temperature of pure mixed solids from 700 to 900 °C. The above results showed that both temperature and doping with ZnO much enhanced the $NiFe_2O_4$ formation, but the thermal action up to 900 °C is more pronounced than the doping action due to limited solubility of ZnO in both oxides lattices up to 900 °C.

The X-ray diffractograms of pure and doped mixed solids calcined at 1000 °C (Fig. 3), 1050 °C (not given here) and 1100 °C (Fig. 4) consisted of the characteristic lines of α-$Fe_2O_3$, NiO and $NiFe_2O_4$ phases. Inspection of Table 1 revealed that the rise in temperature of thermal treatment much enhanced the solid–solid interaction between NiO and α-$Fe_2O_3$ producing $NiFe_2O_4$ because the *R* value increases from 2.2 to 6.94 by increasing the calcination temperature from 1000 to 1100 °C. On the other hand, doping of the investigated system with variable amounts of ZnO (0.75–6 mol%) followed by calcination at 1000–1100 °C (Figs. 3 and 4, Table 1) led to gradual decrease in the peak height of the characteristic lines of α-$Fe_2O_3$ phase (2.69 Å) with subsequent increase in the characteristic lines of $NiFe_2O_4$ (2.95 and 4.82 Å). Table 1 shows that for the pure and doped mixed oxide solids precalcined at 1000–1100 °C, the (*R*) ratio increases progressively as a function of the

Table 1
The effect of precalcination temperature and doping on the height of some diffraction lines at *d*-spacing of 2.51 Å (100% $NiFe_2O_4$ and 50% $Fe_2O_3$), 2.69 Å (100% $Fe_2O_3$) and 2.95 Å (30% $NiFe_2O_4$)

| Solid | Calcination temperature (°C) | Peak height (a.u) | | *R*, 2.51/2.69 | Peak height (a.u), 2.95 Å |
|---|---|---|---|---|---|
| | | 2.51 Å | 2.69 Å | | |
| $NiO–Fe_2O_3$ | 700 | 74 | 102 | 0.725 | – |
| $NiO–Fe_2O_3$ + 0.75% ZnO | 700 | 82 | 100 | 0.82 | – |
| $NiO–Fe_2O_3$ + 1.5% ZnO | 700 | 68 | 83 | 0.82 | – |
| $NiO–Fe_2O_3$ + 3% ZnO | 700 | 50 | 60 | 0.82 | – |
| $NiO–Fe_2O_3$ + 6% ZnO | 700 | 43 | 52 | 0.83 | – |
| $NiO–Fe_2O_3$ | 900 | 106 | 74 | 1.43 | 24 |
| $NiO–Fe_2O_3$ + 0.75% ZnO | 900 | 115 | 76 | 1.51 | 26 |
| $NiO–Fe_2O_3$ + 1.5% ZnO | 900 | 112 | 71 | 1.58 | 28 |
| $NiO–Fe_2O_3$ + 3% ZnO | 900 | 110 | 70 | 1.56 | 28 |
| $NiO–Fe_2O_3$ + 6% ZnO | 900 | 106 | 68 | 1.57 | 28 |
| $NiO–Fe_2O_3$ | 1000 | 150 | 68 | 2.2 | 34 |
| $NiO–Fe_2O_3$ + 0.75% ZnO | 1000 | 192 | 74 | 2.6 | 45 |
| $NiO–Fe_2O_3$ + 1.5% ZnO | 1000 | 177 | 62 | 2.86 | 60 |
| $NiO–Fe_2O_3$ + 3% ZnO | 1000 | 165 | 53 | 3.11 | 75 |
| $NiO–Fe_2O_3$ + 6% ZnO | 1000 | 124 | 34 | 3.65 | 115 |
| $NiO–Fe_2O_3$ | 1050 | 149 | 44 | 3.39 | 45 |
| $NiO–Fe_2O_3$ + 0.75% ZnO | 1050 | 169 | 44 | 3.8 | 58 |
| $NiO–Fe_2O_3$ + 1.5% ZnO | 1050 | 156 | 40 | 4.05 | 67 |
| $NiO–Fe_2O_3$ + 3% ZnO | 1050 | 150 | 33 | 4.48 | 84 |
| $NiO–Fe_2O_3$ + 6% ZnO | 1050 | 140 | 26 | 5.4 | 123 |
| $NiO–Fe_2O_3$ | 1100 | 243 | 35 | 6.94 | 65 |
| $NiO–Fe_2O_3$ + 0.75% ZnO | 1100 | 290 | 30 | $\infty$ | 78 |
| $NiO–Fe_2O_3$ + 1.5% ZnO | 1100 | 290 | 28 | $\infty$ | 88 |
| $NiO–Fe_2O_3$ + 3% ZnO | 1100 | 275 | 25 | $\infty$ | 99 |
| $NiO–Fe_2O_3$ + 6% ZnO | 1100 | 238 | 19 | $\infty$ | 130 |

amount of ZnO dopant. This reflected the role of ZnO doping in enhancing the solid–solid interactions between $\alpha$-$Fe_2O_3$ and NiO with the production of $NiFe_2O_4$ crystalline phase. It is seen from Table 1 that the height of the line at *d*-spacing 2.69 Å (100% $\alpha$-$Fe_2O_3$) for pure and doped samples heated in air at 1100 °C are 35 and 19 (a.u.), respectively. This means that there is a residual amount of $\alpha$-$Fe_2O_3$ phase, i.e. the reaction between NiO and $\alpha$-$Fe_2O_3$ was not completed by heating the reacting solids at 1100 °C for 6 h. The complete conversion of these solids into $NiFe_2O_4$ required a prolonged heating $\geq$24 h at elevated temperatures $\geq$1100 °C [9].

## 4. Discussion

$Fe_2O_3$ and NiO undergo solid–solid interaction to produce $NiFe_2O_4$ that covers the grains of reacting oxides [9,10,33,34]. However, the propagation of this solid–solid interaction to reach completion requires the thermal treatment of the mixed solids at elevated temperatures $\geq$1100 °C [9], to overcome the diffusion of the reacting species through the early formed $NiFe_2O_4$ film covering the surface of grains of NiO and $\alpha$-$Fe_2O_3$ solids. Similar results have been reported in the NiO/$Fe_2O_3$ system doped $Li_2O$ [10,36] and $Al_2O_3$ [34]. Although lithia and alumina stimulated the $NiFe_2O_4$ formation they were incapable of effecting complete conversion of the reacting oxides into nickel ferrite even by precalcination at 1100 °C [9,10,31,33,34,36].

Zinc oxide can be dissolved in the lattice of each of $Fe_2O_3$ and NiO. The dissolution of $Zn^{2+}$ ions in the lattice of NiO or $Fe_2O_3$ solids can proceed via substitution of some of host $Ni^{2+}$ or $Fe^{3+}$ ions and also by location in interstitial position. The dissolution process can be simplified by the use of Kröger's notations

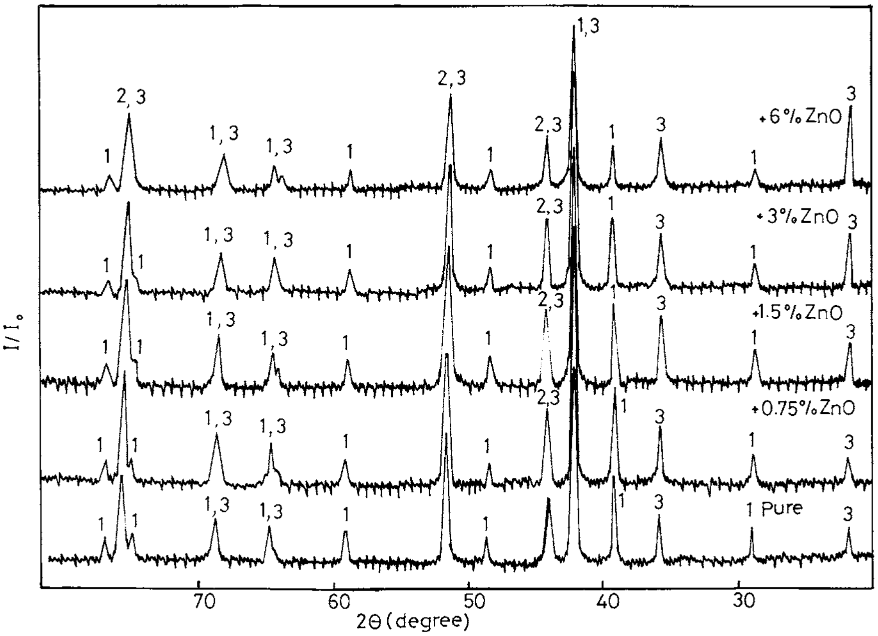

Fig. 3. X-ray diffractograms of pure and doped solids precalcined at 1000 °C. Lines (1) α-$Fe_2O_3$, (2) NiO and (3) $NiFe_2O_4$.

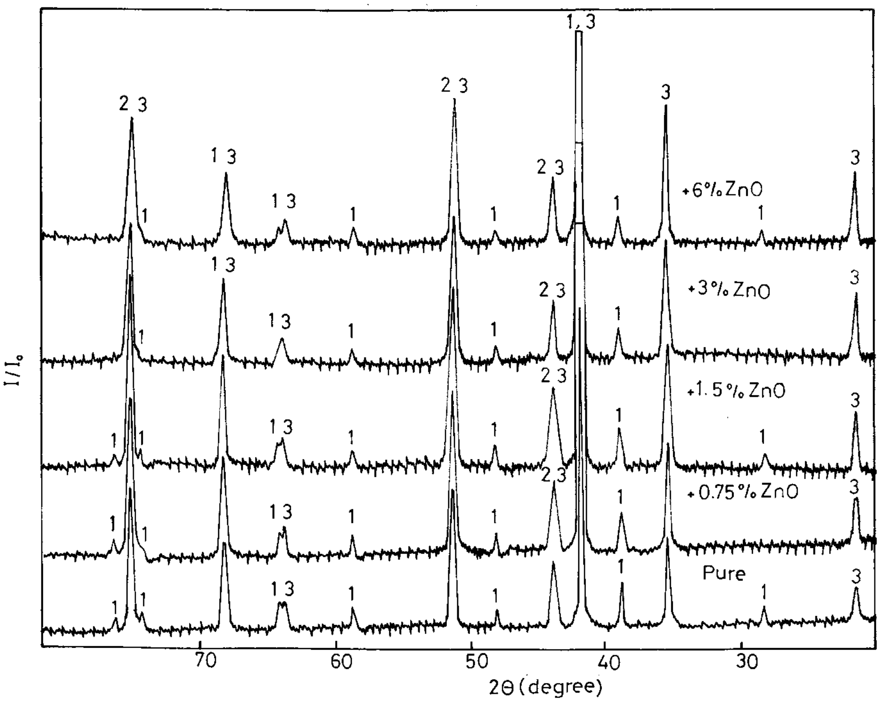

Fig. 4. X-ray diffractograms of pure and doped solids precalcined at 1100 °C. Lines (1) α-$Fe_2O_3$, (2) NiO and (3) $NiFe_2O_4$.

[37] in the following manner:

$$Zn^{2+} + Ni^{2+} \rightarrow Zn(Ni^{2+}) \qquad (1)$$

$$2Zn^{2+} + 2Ni^{2+} \rightarrow 2Zn_{\Delta} + 2Ni^{2+} + CV \qquad (2)$$

$$2Zn^{2+} + 2Fe^{3+} \rightarrow 2Zn(Fe^{3+}) + AV \qquad (3)$$

$$Zn^{2+} + 2Fe^{3+} \rightarrow Zn_{\Delta} + 2Fe^{2+} + \tfrac{1}{2}O_2 \qquad (4)$$

$Zn(Ni^{2+})$ and $Zn(Fe^{3+})$ are divalent zinc ions located in the position of $Ni^{2+}$ and $Fe^{3+}$ of NiO and $Fe_2O_3$ lattices, respectively; CV and AV the created cationic and anionic vacancies, respectively; $Zn_{\Delta}$ the divalent zinc ions retained in interstitial position in NiO and $Fe_2O_3$ lattices (Eqs. (2) and (4)). Reactions (1) and (3) indicate the dissolution of $2Zn^{2+}$ in NiO and $2Zn^{2+}$ in $\alpha$-$Fe_2O_3$ lattices via substitution mechanism.

Location of $Zn^{2+}$ ions in the interstitial positions of NiO lattice lead to formation of cationic vacancies and not to reduction of $Ni^{3+}$ to $Ni^{2+}$ because NiO is stoichiometric at the employed temperature, i.e. no $Ni^{3+}$ ions are present in the lattice.

The dissolution of ZnO in NiO and $\alpha$-$Fe_2O_3$ according to reactions (2) and (3) is expected to be accompanied by an increase in the mobility of $Ni^{2+}$ and $Fe^{3+}$ cations due to creation of cationic and anionic vacancies, respectively. The dissolution of ZnO in NiO and $\alpha$-$Fe_2O_3$ lattices according to Eqs. (1) and (4) is followed by reduction in the concentration of the divalent nickel cations and trivalent iron ions involved in the formation of $NiFe_2O_4$. So, reactions (2) and (3) enhance the solid–solid interactions between the free oxides with production of $NiFe_2O_4$. While, reactions (1) and (4) suppress the propagation of this reaction.

Doping of NiO/$Fe_2O_3$ system with ZnO might lead to dissolution of most of $Zn^{2+}$ ions (ionic radius = 0.74 Å) in NiO lattice (ionic radius = 0.74 Å) mainly via substitution mechanism (Eq. (1)). Location of $Zn^{2+}$ ions of this large size in interstitial position of either NiO or $Fe_2O_3$ is difficult and limited amount of ZnO might dissolve in $Fe_2O_3$ lattice (ionic radius = 0.64 Å) which lead to an effective increase in the mobility of $Fe^{3+}$ ions (Eq. (3)). This speculated preferential dissolution of ZnO in NiO lattice rather than in $Fe_2O_3$ lattice may explain why $ZnFe_2O_4$ was not formed although the chemical affinity of $ZnFe_2O_4$ formation is higher than that of $NiFe_2O_4$ and $Zn^{2+}$ ions act as dopant and have an effective role in increasing the mobility of $Fe^{3+}$ ions and the $NiFe_2O_4$ formation.

The supposed increase in the mobility of the reacting cations could be investigated by determination of the activation energy of formation of $NiFe_2O_4$ phase ($\Delta E$) at temperatures ranging between 1000 and 1100 °C for pure and doped mixed solids, respectively. This has been tentatively achieved by assuming the height of the characteristic diffraction line at 2.95 Å (last column in Table 1) as a measure of the amount of $NiFe_2O_4$ present in a given solid sample at a definite temperature ($T$). By plotting the peak height of this line versus $1/T$, a straight line is obtained whose slope determines $\Delta E$ value by direct application of the Arrhenius equation (Fig. 5). The computed $\Delta E$ values are 103, 85, 70, 41 and 20 kJ mol$^{-1}$ for pure mixed solid sample and those doped with 0.75, 1.5, 3 and 6 mol% ZnO, respectively. This decrease in $\Delta E$ value due to doping process might reflect an effective role of ZnO in increasing the mobility of reacting cations. These findings were in fairly good agreement with the results reported by El-Shobaky et al. [34,36]. It has been reported by these authors that doping of NiO/$Fe_2O_3$ system with 5 mol% $Li_2O$ resulted in a decrease in the activation energy of formation of $NiFe_2O_4$ from 104 to 64 kJ mol$^{-1}$. They have reported also that doping the same system with 10 mol% $Al_2O_3$ resulted in a decrease in $\Delta E$ value from 112 to 68 kJ mol$^{-1}$. The comparison of these results with those given in the present work clearly indicates that the doping of NiO/$Fe_2O_3$ system with 6 mol% ZnO is more efficient in stimulating $NiFe_2O_4$ formation. In fact, the reported $\Delta E$ value for $NiFe_2O_4$ formation due to doping with 6 mol% ZnO effected a decrease in $\Delta E$ value from 103 to 20 kJ mol$^{-1}$.

For lithia, it is highly soluble in NiO lattice, which dissolves more than 11 mol% $Li_2O$. This process which increased the mobility of nickel cations facilitating thus the nickel ferrite formation but effected the conversion of some of $Ni^{2+}$ into $Ni^{3+}$ ions which do not contribute in the ferrite formation. On the other hand, the chemical affinity of $Li_2O$ to react with $Fe_2O_3$ forming $\alpha$- and/or $\beta$-$LiFe_5O_8$ [10,35] is high and it was detected at temperatures starting from 800 °C. These findings can explain the limited role of $Li_2O$ in Ni $Fe_2O_4$ formation.

Alumina enhanced the nickel ferrite formation similar to $Li_2O$ to a limited extent. Although doping of the investigated system with variable amounts of $Al_2O_3$ led to formation of cationic vacancies in NiO lattice

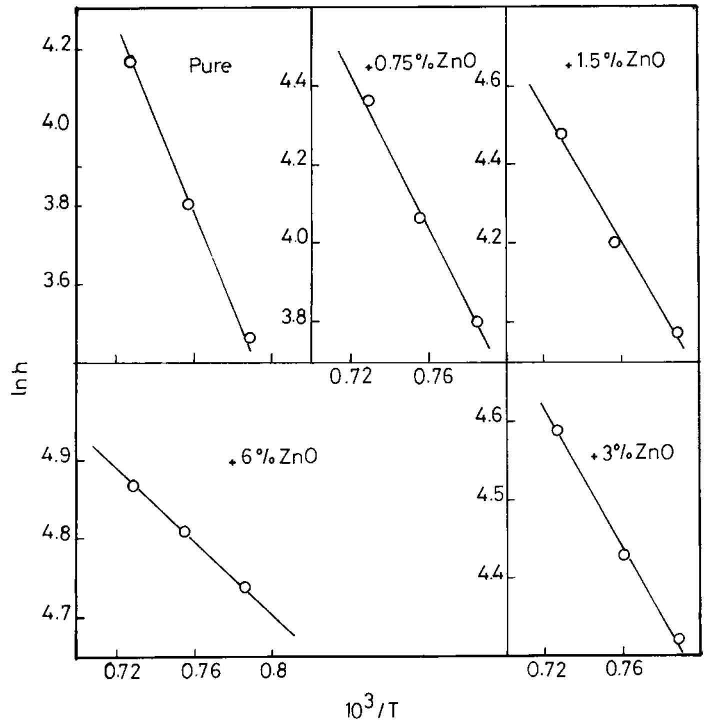

Fig. 5. Change of ln peak height of diffraction line of $NiFe_2O_4$ (2.94 Å) as a function of $1/T$ for pure and ZnO-doped mixed solids.

which increase the mobility of $Ni^{2+}$ ions, but interring of it in $Fe_2O_3$ lattice via substitution or location in interstitial positions might be accompanied by decrease in the trivalent iron reacting cations required in the ferrite formation. Since the role of ZnO in stimulation of $NiFe_2O_4$ formation is more pronounced at temperatures starting from 1000 °C, it can be concluded that ZnO not only effectively increase the mobility of the reacting cations but also other parameter(s) may contribute in such stimulation effect. These parameters arise at temperature starting from 1000 °C. Below this temperature (700–900 °C) the increase in the mobility of reacting cations is the main factor affecting on stimulation of $NiFe_2O_4$ formation. In fact, $Zn^{2+}$ can easily be dissolved in $NiFe_2O_4$ lattice via substitution of some of its $Ni^{2+}$ cations forming $Ni_{1-x}Zn_xFe_2O_4$. The formation of mixed ferrites takes place at temperature starting from 1000 °C according to

$$NiFe_2O_4 + xZnO \xrightarrow{1000\,^{\circ}C} Ni_{1-x}Zn_xFe_2O_4 + xNiO$$

This speculation is confirmed with the results of $CuO/Fe_2O_3$ system doped with ZnO previously published [38]. It was found that ZnO enhanced the $CuFe_2O_4$ formation at temperature starting from 700 °C. The enhancement of ferrite formation at temperatures between 900 and 1000 °C was accompanied by an increase in the peak height of the characteristic diffraction lines of CuO as a function of ZnO added. This increase in the peak heights of CuO lines might indicates substitution of increasing amounts of copper species by zinc species of forming mixed ferrites lattice of formula $Cu_{1-x}Zn_xFe_2O_4$. In the present work it is difficult to talk about the characteristic diffraction lines of NiO phase, firstly because the lines of high intensity are common with $NiFe_2O_4$. Secondly, the observed enhancement in nickel ferrite due to entering of $Zn^{2+}$ ions in the ferrite lattice forming mixed ferrites is the predominant one.

The presence of $Zn^{2+}$ ions in the early formed ferrite lattice increase the diffusion of the reacting cations through the ferrite film covering the surface of grains of NiO and $Fe_2O_3$ solids which acted as an energy barrier, and so decrease the activation energy of nickel ferrite formation.

## 5. Conclusions

The main conclusions that can be derived from the obtained results are:

1. Treatment of equimolar proportions of basic nickel carbonate and ferric oxide with $Zn(NO_3)_2$ (0.75–6 mol%) much enhanced both the degree and rate of decomposition of nickel carbonate to an extent proportional to its amount added.
2. Solid interaction between $\alpha$-$Fe_2O_3$ and NiO occurred at temperatures starting from 700 °C to produce $NiFe_2O_4$. The degree of reaction propagation was increased as a function of temperature.
3. ZnO-doping enhanced the formation of nickel ferrite to a limited extent upon heating at temperature up to 900 °C. The enhancement of nickel ferrite formation upon, doping with variable amounts of ZnO and heating at temperatures between 1000 and 1100 °C was much more pronounced as a function of ZnO added.
4. The completion of solid–solid interactions yielding $NiFe_2O_4$ required prolonged heating of pure or doped mixed oxide solids at elevated temperatures >1100 °C.
5. The activation energy of formation of $NiFe_2O_4$ was determined for pure and ZnO-doped solids and found to be 103, 85, 70, 41 and 20 $kJ\,mol^{-1}$ for pure solids and those doped with 0.75, 1.5, 3 and 6 mol%, respectively.

## References

[1] G. Busca, E. Finocchio, V. Lorenzelli, M. Trombetta, S.A. Rossini, J. Chem. Soc., Faraday Trans. 92 (23) (1996) 4687.
[2] M. Zhang, R. Lan, J. Liu, X. Chen, W. Zhou, J. Chem. Soc., Faraday Trans. 88 (4) (1992) 637.
[3] J. Johan, A.J. Van Dillen, J.W. Geus, J. Chem. Soc., Faraday Trans. 87 (10) (1991) 1623.
[4] B.S. Randhawa, S. Kaur, P.S. Bassi, Indian J. Chem. A 28 (6) (1989) 463.
[5] L. Dong, Z. Liu, Y. Hu, B. Xu, Y. Chen, J. Chem. Soc., Faraday Trans. 94 (19) (1998) 3033.
[6] P. Lahiri, S. Sengupta, Can. J. Chem. 69 (1) (1991) 33.
[7] P. Lahiri, S. Sengupta, J. Chem. Soc., Faraday Trans. 91 (19) (1995) 3489.
[8] N.K. Singh, S.K. Tiwari, K.L. Anitha, R.N. Singh, J. Chem. Soc., Faraday Trans. 92 (13) (1996) 2397.
[9] G.A. El-Shobaky, A.A. Ibrahim, Thermochim. Acta 132 (1988) 117.
[10] G.A. El-Shobaky, G.A. Fagal, A. Abd El-Aal, A.M. Ghozza, Thermochim. Acta 256 (1995) 429.
[11] G.A. El-Shobaky, F.H.A. Abdalla, A.M. Ghozza, Thermochim. Acta 292 (1997) 123.
[12] H.G. El-Shobaky, Thermochim. Acta 343 (2000) 145.
[13] N.R.E. Radwan, H.G. El-Shobaky, Thermochim. Acta 360 (2000) 147.
[14] G.A. El-Shobaky, N.R.E. Radwan, F.M. Radwan, Thermochim. Acta 380 (2001) 27.
[15] J.A. Toledo, M.A. Valenzuela, P. Bosch, H. Armendariz, A. Montoya, N. Nava, A. Vazquez, Appl. Catal. A 198 (2000) 235.
[16] T. Konvicka, P. Mosner, Z. Solc, J. Therm. Anal. Calorim. 60 (2000) 629.
[17] V.M. Bujoreanu, E. Segal, J. Therm. Anal. Calorim. 61 (2000) 967.
[18] T. Sato, K. Haneda, M. Seki, T. Iijima, Proceedings of the International Symposium on Physics of Magnetic Materials, World Scientific, Singapore, 1987, p. 210.
[19] E.P. Wohlfarth (Ed.), Ferromagnetic Materials, North-Holland, Amsterdam, 1980.
[20] P. Mollard, A. Collomb, J. Devenyl, A. Rousset, J. Paris, IEEE Trans. Mag. 11 (1975) 894.
[21] W.J. Schuele, V.D. Deetscreek, J. Appl. Phys. 32 (1961) 235.
[22] M. Kimaya, Bull. Chem. Soc. Jpn. 51 (1978) 134.
[23] K. Matsuda, I. Kayama, Proc. Mac. Sci. Tokai Univ. 17 (1982) 101.
[24] T. Sato, T. Iijima, M. Seki, N. Inagaki, J. Magn. Magn. Mater. 65 (1987) 252.
[25] H. Tamura, E. Matijevic, J. Colloid Interf. Sci. 90 (1982) 100.
[26] R.E. Vandenberghe, R. Valeerberghe, E. Degrave, G. Robbrecht, J. Magn. Magn. Mater. 15–18 (1980) 1117.
[27] G.A. Kolta, S.Z. El-Tawil, A.A. Ibrahim, N.S. Felix, Thermochim. Acta 39 (1980) 359.
[28] A. Feltz, Martin, Mater. Sci. Nonorg. React. Solids 28 (1985) 137.
[29] R.K. Tami, K.K. Kamada, T. Ishci, React. Solids 1 (1980) 309.
[30] F.J.C. Toolenaar, J. Mater. Sci. 24 (1989) 1089.
[31] G.A. El-Shobaky, F.H.A. Abdalla, A.A. Fouad Zikry, Thermochim. Acta 289 (1996) 81.
[32] M. Crisan, D. Crisan, Mater. Sci. Monogr. (Ceram. Powder) 52 (1983) 429.
[33] G.A. El-Shobaky, A.N. Al-Noaimi, A. Abd El-Aal, A.M. Ghozza, Mater. Lett. 2 (1995) 39.
[34] G.A. El-Shobaky, A.A. Ibrahim, Bull. Soc. Chim. France 6 (1989) 34.
[35] G.A. El-Shobaky, M.A. Shouman, M.N. Alaya, Adsorpt. Sci. Technol. 18 (2000) 243.
[36] A.A. Ibrahim, G.A. El-Shobaky, Thermochim. Acta 132 (1988) 117.
[37] F.A. Kröger, Chemistry of Imperfect Crystals, North-Holland, Amsterdam, 1964.
[38] N.A.M. Deraz, Ph.D. Thesis, Zagazig University, Egypt, 1999.